Molecular Human Reproduction, Vol.21, No.2 pp. 169–185, 2015
Advanced Access publication on October 29, 2014 doi:10.1093/molehr/gau099

molecular human reproduction

ORIGINAL RESEARCH

Dpy19l2-deficient globozoospermic sperm display altered genome packaging and DNA damage that compromises the initiation of embryo development

Sandra Yassine[1,2,†], Jessica Escoffier[1,2,†], Guillaume Martinez[1,2], Charles Coutton[1,2,3], Thomas Karaouzène[1,2], Raoudha Zouari[4], Jean-Luc Ravanat[1,5], Catherine Metzler-Guillemain[6,7], Hoi Chang Lee[8], Rafael Fissore[8], Sylviane Hennebicq[1,9], Pierre F. Ray[1,2,10], and Christophe Arnoult[1,2,*]

[1]Université Grenoble Alpes, Grenoble, F-38000, France [2]Equipe 'Andrologie, Génétique et Cancer' Laboratoire AGIM, CNRS FRE3405, La Tronche, F-38700, France [3]CHU de Grenoble, UF de Génétique Chromosomique, Grenoble, F-38000, France [4]Clinique des Jasmins, 23, Av. Louis BRAILLE, 1002 Tunis, Tunisia [5]Laboratoire Lésions des Acides Nucléiques, CEA, INAC-SCIB, F-38000 Grenoble, France [6]Aix-Marseille Université-Inserm UMR 910, Génétique médicale et Génomique Fonctionnelle, 13385 Marseille Cedex 5, France [7]APHM Hôpital La Conception, Gynépôle, Laboratoire de Biologie de la Reproduction – CECOS, 13385 Marseille Cedex 5, France [8]Department of Veterinary and Animal Sciences, University of Massachusetts, Amherst, 661 North Pleasant Street, Amherst, MA 01003, USA [9]CHU de Grenoble, Centre d'AMP-CECOS, BP217, Grenoble Cedex 9, F-38043, France [10]CHU de Grenoble, UF de Biochimie et Génétique Moléculaire, Grenoble, F-38000, France

*Correspondence address. AGIM, Equipe 'Andrologie, Génétique et Cancer', Faculté de Médecine, 38700 La Tronche, France. Tel: +33-4-76-63-74-08; E-mail: christophe.arnoult@ujf-grenoble.fr

Submitted on August 28, 2014; resubmitted on October 13, 2014; accepted on October 24, 2014

ABSTRACT: We recently identified the *DPY19L2* gene as the main genetic cause of human globozoospermia. Non-genetically characterized cases of globozoospermia were associated with DNA alterations, suggesting that DPY19L2-dependent globozoospermia may be associated with poor DNA quality. However the origins of such defects have not yet been characterized and the consequences on the quality of embryos generated with globozoospermic sperm remain to be determined. Using the mouse model lacking Dpy19l2, we compared several key steps of nuclear compaction. We show that the kinetics of appearance and disappearance of the histone H4 acetylation waves and of transition proteins are defective. More importantly, the nuclear invasion by protamines does not occur. As a consequence, we showed that globozoospermic sperm presented with poor sperm chromatin compaction and sperm DNA integrity breakdown. We next assessed the developmental consequences of using such faulty sperm by performing ICSI. We showed in the companion article that oocyte activation (OA) with globozoospermic sperm is very poor and due to the absence of phospholipase Cζ; therefore artificial OA (AOA) was used to bypass defective OA. Herein, we evaluated the developmental potential of embryos generated by ICSI + AOA in mice. We demonstrate that although OA was fully rescued, preimplantation development was impaired when using globozoospermic sperm. In human, a small number of embryos could be generated with sperm from *DPY19L2*-deleted patients in the absence of AOA and these embryos also showed a poor developmental potential. In conclusion, we show that chromatin compaction during spermiogenesis in *Dpy19l2* KO mouse is defective and leads to sperm DNA damage. Most of the DNA breaks were already present when the sperm reached the epididymis, indicating that they occurred inside the testis. This result thus suggests that testicular sperm extraction in Dpy19l2-dependent globozoospermia is not recommended. These defects may largely explain the poor embryonic development of most mouse and human embryos obtained with globozoospermic sperm.

Key words: male infertility / globozoospermia / Dpy19l2 / DNA compaction / protamine

[†] Shared first authorship.

Introduction

The sperm epigenome presents several peculiarities, due to the great compaction of the nucleus during spermiogenesis. Indeed, the sperm genome undergoes a complete chromatin remodeling during post-meiotic differentiation. The most significant of these events are (i) an almost genome-wide removal of histones and their replacement by protamines (Prms), (ii) nucleosome retention at specific genomic loci, likely linked with early paternal gene activation after fertilization (Arpanahi *et al.*, 2009; Hammoud *et al.*, 2009) and (iii) the presence within the sperm of specific small regulating RNAs, known to modulate gene expression and embryo development after fertilization (Dadoune, 2009). It is now recognized that the whole paternal epigenome plays an important role in the developing embryo (Miller *et al.*, 2010; Jenkins and Carrell, 2012). However, although the current literature provides strong evidence for a relationship between male infertility and dysregulation of sperm epigenetic marks (Cho *et al.*, 2001; Oliva, 2006), our knowledge of the role of paternal epigenetic marks during the different steps of embryonic development and their evolution during embryogenesis remains poor. More importantly, the long-term consequences of male epigenetic dysregulation are unknown and may lead to pathological phenotypes in offspring. These questions are highly important for human reproduction because ICSI, necessary to treat teratozoospermic patients, uses sperm which very often present multiple and severe DNA defects. In consequence, efforts should be made to characterize the pathological epigenetic landscape of sperm chromatin (DNA breaks, compaction and epigenetic defects) in the context of male infertility and to understand the etiology of these abnormal profiles.

In the last few years we have focused our attention on a specific type of teratozoospermia, namely globozoospermia (MIM #613958), which is characterized by the presence in the ejaculate of a large majority of round spermatozoa devoid of an acrosome. We demonstrated that genetic defects of *DPY19L2* were identified in >70% of men presenting with globozoospermia indicating that *DPY19L2* represents the main cause of this teratozoospermia (Harbuz *et al.*, 2011; Coutton *et al.*, 2012, 2013). Two other genes are also involved in type I globozoospermia, *SPATA16* and *PICK1*, but with a lower incidence (Dam *et al.*, 2007; Liu *et al.*, 2010). If the absence of an acrosome is the main feature of globozoospermic sperm, previous cases reports have shown that the chromatin of globozoospermic sperm presents defective condensation and DNA alterations (Baccetti *et al.*, 1996; Vicari *et al.*, 2002; Vozdova *et al.*, 2013). These results suggest that Dpy19l2-dependent globozoospermia is also associated with poor sperm DNA quality. However, this hypothesis is based on only a few case descriptions, which were performed without neither the identification of the genetic etiology nor the precise characterization of the DNA alterations. The DNA quality of DPY19L2-dependent globozoospermic sperm remains thus to be assessed. Moreover, the origins of such defects have not been characterized and, finally, the consequences on the quality of embryos generated with DPY19L2-dependent globozoospermic sperm remain to be determined.

Because of the absence of an acrosome in globozoospermic sperm, production of embryos requires the use of ICSI. Indeed, before the development of assisted reproductive techniques (ART), and more particularly ICSI, the treatment of globozoospermia was not possible and affected men remained sterile. Although several teams reported successful pregnancy and offspring from men with globozoospermia using ICSI (Lundin *et al.*, 1994); the overall rate of success of ICSI with globozoospermic sperm remained very low (Liu *et al.*, 1995; Battaglia *et al.*, 1997). In the accompanying report, we demonstrated that the absence of oocyte activation (OA), associated with Dpy19l2-dependent globozoospermic sperm is in fact due to the absence of phospholipase C zeta (PLCζ) (Escoffier *et al.*, companion article). The lack of OA in globozoospermic cases can be circumvented with artificial oocyte activation (AOA) using Ca^{2+} ionophore (Liu *et al.*, 1995; Battaglia *et al.*, 1997; Tejera *et al.*, 2008; Kyono *et al.*, 2009; Taylor *et al.*, 2010). A recent study on DPY19L2-dependent globozoospermic patients showed that AOA rescues fertilization and allows a significantly improved fertilization and delivery rate (Kuentz *et al.*, 2013). However, the delivery rate remains relatively low in cases of ICSI performed with globozoospermic sperm + AOA, reaching 31% (mean female age 29.7 years) (Kuentz *et al.*, 2013) compared with a 45.9% (age <35 years) in a large study of control cohort patients (Palermo *et al.*, 2009), suggesting that embryonic development is somehow defective following conception using globozoospermic sperm. Recently, a *Dpy19l2* knock-out (KO) mouse has become available and its reproductive phenotype is remarkably similar to the human disease: males are completely infertile, with 100% globozoospermic sperm (Pierre *et al.*, 2012). This model therefore represents an opportunity (i) to characterize the DNA quality of Dpy19l2 KO sperm, (ii) to unravel the reasons behind the abnormalities of DNA organization in globozoospermic sperm and (iii) to evaluate the developmental potential of preimplantation embryos conceived with *Dpy19l2*-deficient sperm.

In this paper, using the KO mouse model, we show that several DNA compaction stages are defective. We note in particular that the protamines fail to invade the nucleus during the last stage of compaction leading to a defective nuclear compaction and the occurrence of DNA breaks. This defective compaction largely explains the poor sperm chromatin compaction and sperm DNA integrity breakdown of Dpy19l2-deficient mature sperm. We also show that the development of mouse embryos generated by ICSI and AOA from *Dpy19l2* KO sperm and of human embryos generated by ICSI from sperm of *DPY19L2*-deleted patients were severely impaired. Collectively, our data provide important new insights into the molecular pathogenesis of DPY19L2-dependent globozoospermia, which should lead to improved therapeutic strategies and sheds light on the mechanisms that regulate the organization of the sperm head.

Materials and Methods

Biological samples

Human. Sperm were obtained from patients consulting at the fertility department of Grenoble and Marseille Hospitals (France) or Clinique des Jasmins (Tunis, Tunisia), following approval by the ethical committee and informed consent from the patients. All patients gave an informed consent for the conservation of the remnant sperm in the Germetheque biobank and their use in studies on human fertility in accordance with the Helsinki Declaration of 1975 on human experimentation. The Germetheque Scientific Committee approved the present study design. Globozoospermic patients underwent a genetic analysis as previously described (Harbuz *et al.*, 2011) and homozygously *DPY19L2*-deleted patients were selected. Human sperm were collected by masturbation and washed twice in Dulbecco's phosphate-buffered saline (PBS). All animal procedures were performed according

to French and to IACUC UMASS guidelines on the use of living animals in scientific investigations with the approval of the respective local ethical review committees (Grenoble-Institut des Neurosciences – ethical committee, agreement number 004). *Dpy19l2 KO* mice were obtained from Mutant Mouse Regional Resource Center (MMRRC), University of California, Davis, CA, USA. First, epididymis was isolated and sperm were collected from the different parts of the epididymis (caput, corpus, or cauda) by direct puncture in M2 medium. Sperm were allowed to swim for 10 min and collected by centrifufation at 500 g.

Gradation of human embryos

Grade I embryos had even, regular, spherical blastomeres with $<10\%$ fragmentation; grade II embryos had uneven or irregular blastomeres with $<10\%$ fragmentation; grade III embryos had blastomeres in grade II condition with 10–50% fragmentation and grade IV embryos had $>50\%$ fragmentation or developmental arrest.

Spermatogenic cell preparation

C57BL6 male or *Dpy19l2* KO mice (8 weeks old) were killed by cervical dislocation. The testes were surgically removed and placed in PBS (at room temperature). The tunica albunigea was removed from the testes with sterile forceps and discarded. Then, the testes were incubated in 1 mg/ml of collagenase solution in EKRB cell buffer containing in mM 2 $CaCl_2$, 12.1 Glucose, 10 HEPES, 5 KCl, 1 $MgCl_2$, 6 Na-Lactate, 150 NaCl, 1 NaH_2PO_4, 12 $NaHCO_3$ pH 7, and agitated horizontally at a maximum of 120 rpm for 30 min at 25°C. The dispersed seminiferous tubules were then washed with PBS and cut thinly. Cells were dissociated by gently pipetting, filtered through a 100 μm filter and then pelleted by centrifugation at 500 g for 10 min. Cells were suspended in 1 ml PBS, fixed with 4% paraformaldehyde (PFA) solution, washed with PBS and finally layered onto polylysine-coated slides.

Collection of gametes for ICSI

Sperm from caudae epididymides of different mouse strains (*Dpy19l2* KO and WT B6D2F1) were allowed to swim for 10 min at 37°C in 1 ml of NIM medium containing (in mM) KCl 125, NaCl 2.6, Na_2HPO_4 7.8, KH_2PO_4 1.4 and EDTA 3 (pH 7.0). Sperm were then washed twice by centrifugation at 500 g with NIM medium, then resuspended in 100 μl NIM + 12% PVP (PVP360 sigma) medium. The sperm head was separated from the tail by the application of several piezo pulses (PiezoXpert®, Eppendorf) or by sonication (2 × 15 s).

Oocyte preparation

B6D2F1 female mice, 7–11 weeks old, were superovulated by IP injection of 7.5 IU pregnant mare's serum gonadotrophin (PMSG; Intervet) followed by 7.5 IU HCG (Intervet) 48 h later. Oocytes were collected from oviducts about 14 h after hCG injection. Cumulus cells were removed with 0.1% bovine testicular hyaluronidase (300 USP U/mg; ICN Biochemicals, Costa Mesa, CA, USA) in M2 medium for 5–10 min. Oocytes were rinsed thoroughly and kept in M2 at 15°C for at least 15 min until required for ICSI.

Media

M2 medium (Sigma) and CZB.HEPES (CZB.H, in mM) (HEPES 20, NaCl 81.6, KCl 4.8, $MgSO_4$ 1.2, $CaCl_2$ 1.7, KH_2PO_4 1.2, EDTA.Na_2 0.1, Na-lactate 31, $NaHCO_3$ 5, Na-pyruvate 0.3, polyvinyl alcohol 0.1 mg/ml, phenol red 10 mg/ml (0.5% (w/v) in DPBS), pH 7.4) was used for gamete handling and ICSI in air. KSOM (100×, Life technologies) supplemented with 1% essential amino acids (100×, Life technologies) were used for embryo culture (KSOM/EAA).

ICSI procedures

ICSI was performed according to the method described by Yoshida and Perry (2007). For microinjection, sperm were stored in 50 μl of NIM, 12% PVP medium supplemented with 0.3 μg/μl of complementary RNA (cRNA) PLCζ depending on the experimental design and moved directly to the injection chamber. Sperm were introduced into the ooplasm using micromanipulators (Micromanipulator InjectMan®, Eppendorf) mounted on an inverted Nikon TMD microscope. The sperm suspension was replaced every 30 min during the ICSI experiment. Oocytes that survived the ICSI procedure were incubated in KSOM/EAA medium at 37°C under an atmosphere of 5% CO_2. Pronucleus formation was checked at 6 h after ICSI, and outcomes were scored up to the blastocyst stage.

Parthenogenetic oocyte activation experiments

Oocytes were activated by injection of cRNA PLCζ (0.3 μg/μl, concentration in the pipette) into the ooplasm or by incubating them in Ca^{2+}-free CZB supplemented with 10 mM SrCl for 2 h at 37.5°C in a humidified incubator with 5% CO2. After Sr^{2+} treatment or cRNA microinjection, oocytes were cultured in KSOM/EAA. The media for Sr^{2+} activation was supplemented with 5 μg/mL cytochalasin B (CB) to prevent second polar body extrusion and diploidize the parthenotes. The cRNA PLCζ injection volume was 5–10 pl, which is ~1–3% of the total egg volume. Pronucleus formation was checked at 6 h after ICSI, and outcomes were scored up to the blastocyst stage.

Messenger RNA preparation

Complementary DNA (cDNA) encoding for full-length mouse PLCζ1 (GenBank Accession number AF435950; a gift from K. Fukami, Tokyo University of Pharmacy and Life Science, Tokyo, Japan) was amplified by PCR and cloned into the pCS2+ vector. In brief, the cDNA was linearized at the NotI site, and transcribed *in vitro* using the mMessage/mMachine capping kit (Ambion, Austin, TX, USA). Capped and poly(A)-tailed cRNAs were purified from the reaction mixture using the MEGAclear Kit (Ambion). The cRNAs were eluted with diethylpyrocarbonate-treated H2O and, if necessary, further diluted with it before microinjection.

Immunofluorescence and histology

Testes were fixed for 24 h in 4% PFA. Tissue was dehydrated in a graded ethanol series, embedded in paraffin (Leica TP1020 and EG1150) and sectioned (4 μm thickness) onto slides (Leica RM2245). For histology studies, sections were stained via an automated slides stainer (Leica Autostainer XL V2.2). For immunohistochemistry, heat antigen retrieval was performed by boiling slides immersed in 0.01 M sodium citrate buffer, 0.05% Tween 20, pH 6.0 for ~25 min. For sperm immunofluorescence studies, sperm were fixed with in PBS/4% PFA for 1 min at room temperature. After washing in 1 ml PBS, the sperm suspension was spotted onto 0.1% poly L-lysine precoated slides (Thermo Scientific). After attachment, sperm or spermatogenic cells were permeabilized with 0.1% (v/v) Triton X-100–DPBS (Triton X-100; Sigma-Aldrich) for 5 min at room temperature. Slides were then blocked in the corresponding 5% normal serum–DPBS (normal goat or donkey serum; GIBCO, Invitrogen) and incubated overnight at 4°C with primary antibodies. For Prm1 and Prm2 detection, heat antigen retrieval was associated with DNA decondensation in 10 mM Dithiothreitol, 0.1 M Tris–HCl (pH 8.0) for 1 h at room temperature. After decondensation, the slides were washed twice in deionized water before starting immunofluorescence experiments. Washes were performed with 0.1% (v/v) Tween 20–DPBS, followed by 1 h incubation at room temperature with Alexa Fluor 555-labeled goat anti-rabbit or Dylight 488-labeled goat anti-rabbit (1:400) secondary antibodies. Samples were counterstained with

5 μg/ml Hoechst 33342 and mounted with DAKO mounting media (Life technology). Control sections were incubated with PBS containing 0.1% Triton and the corresponding normal serum without the primary antibody.

Fluorescence images were captured with confocal microscopy (Zeiss LSM 710) outfitted with a 63× oil immersion objective for mice sperm and 100× oil immersion objective for human sperm and analyzed with ZEN lite software (Zeiss). Whole images were reconstructed and projected from Z-stack images using ZEN software.

Primary antibodies

Mouse Sperm Protein sp56 Monoclonal Antibodies were from QED Bioscience; Acetyl histone H4 antibodies (06-598) were from Millipore; Protamine 1 (sc-23107), Protamine 2 (sc-23104) and Tnp2 Antibodies (sc-21106) were from Santa Cruz. Tnp1 antibody (ab73135) was from Abcam. Antibodies were used at the following concentration anti-Tnp1, 1/1000; anti-Tnp2, 1/100; anti-Acetylated Histone, H4 1/100, anti-Prm1 and Prm2, 1/100.

Chromomycin A_3 staining

Semen samples were washed twice with 5 ml of PBS 1× and fixed in a methanol/acetic acid (3:1,v/v) solution at 4°C for at least 30 min. Cells were spread on Superfrost© slides and air dried at room temperature overnight. Cells were labeled using a 0.25 mg/ml chromomycin A_3 (CMA_3) solution in McIlvaine buffer (pH 7) for 20 min, and washed two times for 2 min with McIlvaine buffer. Sperm nuclei were counterstained in a 0.5 μg/ml Hoechst solution for 3 min, washed in PBS for 3 min and mounted with DAKO mounting media. Slides were analyzed using a fluorescent microscope (Nikon Eclipse 80i).

Aniline blue

Semen samples were washed twice with 5 ml of PBS 1×, 10 μl were spread on a slide, allowed to air dry and then fixed with a 3% glutaraldehyde solution in PBS 1× for 30 min at room temperature. Slides were then incubated 5 min in water, 10 min in 5% aniline blue diluted in 4% acetic acid solution, two times for 2 min in water, 2 min in 70, 90 and 100% ethanol solutions and finally 2 min in Toluene. Slides were then analyzed using a microscope with a transmitted light microscope 100× objective with oil.

Oxidative DNA damage

Quantification of 8-oxo-7,8-dihydro-2′-deoxyguanosine (8-OHdG) was performed by isotope dilution high-performance liquid chromatography-electrospray tandem mass spectrometry assay, as previously described (Ravanat *et al.*, 1998). DNA was extracted as previously described with an optimized protocol that minimizes DNA oxidation during the work-up (Badouard *et al.*, 2008).

DNA breaks

Semen samples were washed twice with 5 ml of PBS and fixed in a methanol/acetic acid (3:1,v/v) solution at 4°C for at least 30 min. Cells were spread on Superfrost© slides and air dried at room temperature overnight. Cells were permeabilized using 0.1% (v/v) Triton X-100, 0.1% (w/v) sodium citrate in PBS 1× for 2 min and labeled by terminal deoxynucleotidyl transferase mediated deoxy-UTP nick end labeling (TUNEL) according to the Roche protocol of the In Situ Cell Detection Kit (Roche Diagnostic, Manheim, Germany). Sperm nuclei were counterstained in a 0.5 μg/ml Hoechst solution for 3 min, washed in PBS for 3 min and mounted with DAKO mounting media. Slides were analyzed using a fluorescent microscope (Nikon Eclipse 80i).

Statistical analyses

Statistical analyses were performed with SigmaPlot using the Student's *T*-test. Data presented represent mean ± SE. Statistical tests with a two-tailed *P*-values ≤ 0.05 were considered as statistically significant.

Results

Dpy19l2 KO spermatid chromatin compaction is defective and shows defective transport of protamines into the nucleus

We first studied in detail the main stages of spermatid DNA compaction in WT and globozoospermic sperm. The replacement of histone by protamine is a complex process, involving first histone post-translational modifications and the incorporation of testis-specific variants (Montellier *et al.*, 2013), leading to nucleosome instability. One of the best characterized histone modifications, which occurs at the beginning of the spermatid elongation stage, is a wave of hyperacetylation affecting core histones (Hazzouri *et al.*, 2000), including H4, which has been later demonstrated to interact with Brdt, the testis-specific member of the double bromodomain containing proteins of the BET family, which controls the histone-to-transition proteins and protamine exchange (Gaucher *et al.*, 2012). Histone acetylation was measured in testis sections of WT and *Dpy19l2* KO mice by observing the staining pattern obtained by the binding of an antibody raised against acetylated histone H4 (H4ac). No difference was measured between the H4 acetylation waves of WT and KO elongating spermatids from tubule sections at stage IX, where H4ac is homogeneously distributed throughout the whole nucleus (Fig. 1A–D). During the elongation of spermatids, acetylated core histones are transiently replaced by a set of two basic proteins named nuclear transition proteins 1 and 2 (Tnp1 and Tnp2). In elongating/condensing spermatids from WT tubule sections at stages X-XI, histone replacement is partial (Hazzouri *et al.*, 2000) and a subset of nucleosomes retained H4acs located at the base of the sperm head, close to the flagellum (Fig. 1E, white arrows). In contrast, in *Dpy19l2* KO spermatids, most of the spermatids presented no obvious polarization, with H4ac staining surrounding the nucleus (Fig. 1F, white arrows), suggesting that their replacement and removal was performed but according to a different axis. This difference is likely due to the defective manchette (Pierre *et al.*, 2012) leading to a disturbance of protein trafficking in *Dpy19l2* KO spermatids. The next stage involved the nuclear transition proteins Tnp1 and Tnp2, which play crucial roles in sperm DNA compaction, and also in flagellum biogenesis (Zhao *et al.*, 2004). The arrival of Tnp1 and Tnp2 into the nucleus of elongated spermatids during compaction was observed in both WT and *Dpy19l2* KO tubule sections at stages IX and X and no difference was found between the two genotypes (Fig. 2), suggesting that histone replacement by transition proteins occurred normally. In a preparation of dissociated WT spermatogenic cells, we observed a progressive incorporation of Tnp proteins into the nucleus from the base to the apex during the spermatid compaction (Fig. 3A–C). The disappearance and replacement of Tnps then seemed to start first at the center of the nucleus and next take place at the nucleus border (Fig. 3D). This observed pattern of Tnps replacement is consistent with Tnps replacement in rat spermatids (Kolthur-Seetharam *et al.*, 2009). Again, the absence of elongation in *Dpy19l2* KO spermatids disturbed the specific pattern of Tnps assembly/

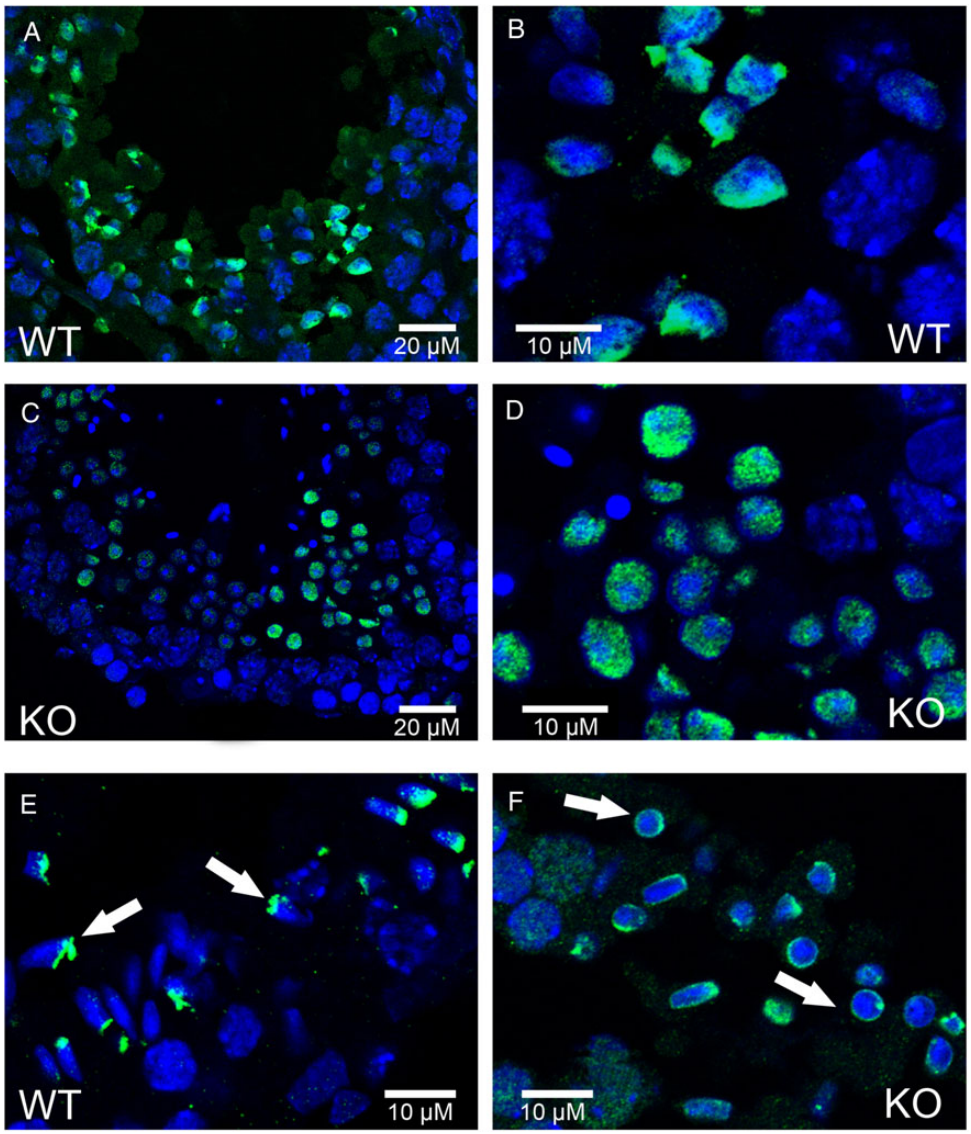

Figure 1 Histone H4 is acetylated in both WT and *Dpy1912* KO testis sections, but present different pattern of vanishing. (**A**–**F**) Testis sections were fixed and stained with Hoechst to mark DNA (blue) and with antibodies targeting acetylated histone H4 (H4ac, green signal). (A and B) Wild type (WT) testis sections showing H4 acetylation on late round spermatids. (C and D) Testis section from *Dpy1912* knock-out (KO) males showing H4 acetylation on late round spermatids. (E) WT testis sections showing the localization of H4ac on elongating spermatids (white arrows). (F) Testis section from *Dpy1912* KO males showing the localization of H4ac on condensed spermatids, which likely corresponded to WT elongated spermatids.

removal, as observed in WT spermatids (Fig. 3F–H). However, no dramatic alteration of Tnps assembly/removal was observed in *Dpy1912* KO spermatids, which strongly suggests that Tnp-dependent compaction is partially affected at this stage. In a last poorly understood step, Tnps are then replaced by protamines, which eventually allow the compaction of sperm DNA by ~10-fold. Protamine localization was observed in epididymal sperm. Remarkably, *Dpy1912* KO sperm cells presented a dramatic loss of protamines: both protamines formed a ring at the nucleus periphery (Fig. 4A and B). In contrast, protamines were present in the whole nucleus of WT sperm, with a stronger staining in the apex (Fig. 4C and D). In addition, epididymal *Dpy1912* KO sperm presented other defects. First, contrary to WT sperm, H4ac histone was still present but with an unexpected location in the midpiece (Fig. 4E and F). Second, both Tnps were still present in this stage, as a ring surrounding the nucleus, whereas Tnps are normally absent in mature WT sperm (Fig. 4G–J). We want to point out that we observed a small specific staining at the flagellum insertion in the head for Tnp1 (Fig. 4I, white arrow heads). Such a specific staining was not observed for Tnp2 (Fig. 4J).

Mature Dpy1912-dependent globozoospermic mouse and human sperm present positive acidic aniline blue and CMA_3 tests

In fertility clinics, DNA compaction of ejaculated sperm is evaluated by two complementary tests: the acidic aniline blue (and the CMA_3 tests, which are positive when histones are retained inside the nucleus and

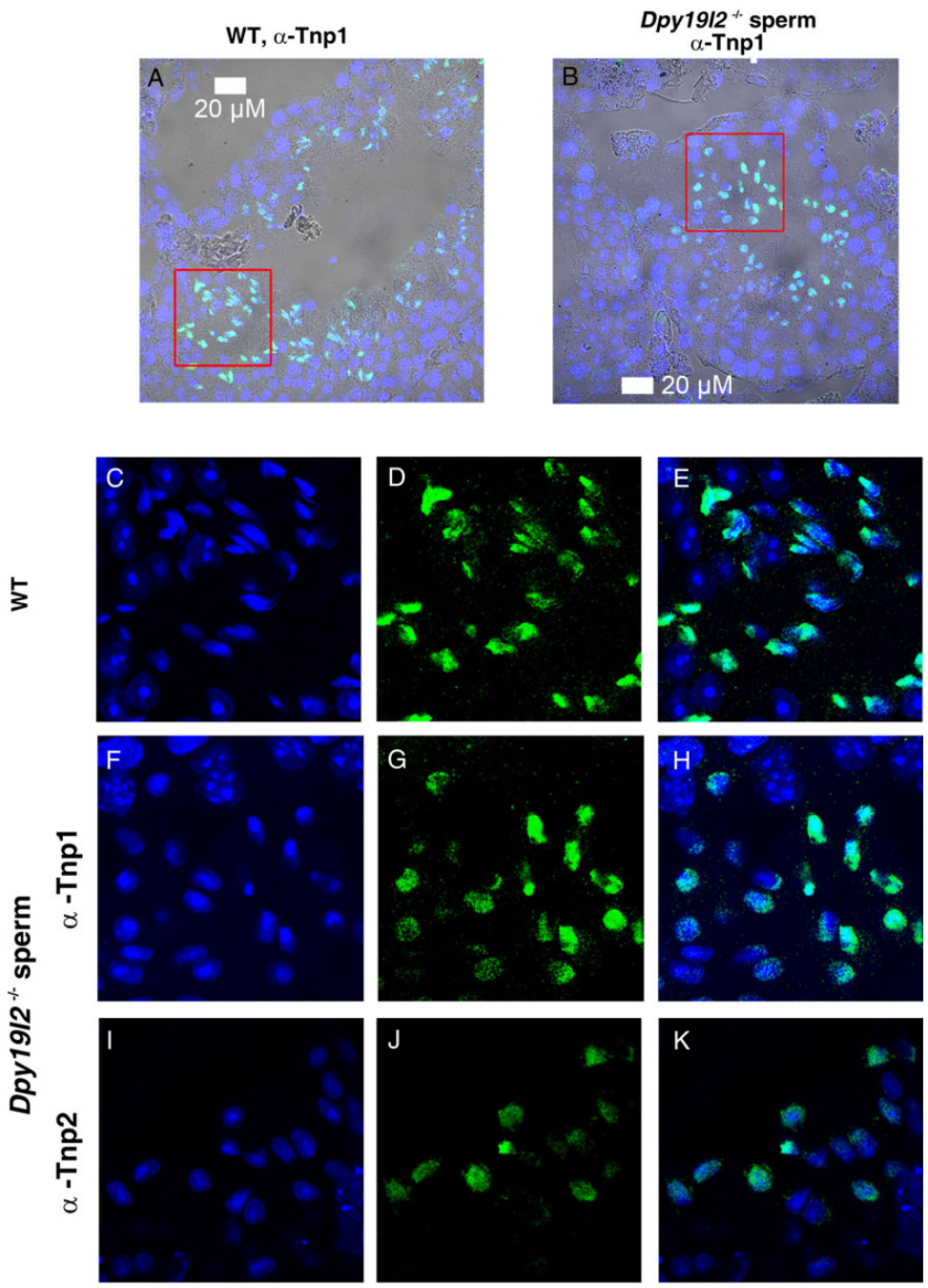

Figure 2 Tnp1 and Tnp2 nuclear localizations are similar in WT and *Dpy19l2* KO testis sections. (**A** and **B**) Testis sections are stained with antibody against transition protein (Tnp)1 and Hoechst. Overlay of Hoechst, Tnp1 staining and phase contrast. Left WT and right *Dpy19l2* KO sperm. (**C**–**E**) Enlargement of the red square drawn in (A) (full size 60 μM × 60 μM). From left to right Hoechst, Tnp1 staining and Overlay. (**F**–**H**) Enlargement of the red square drawn in (B) (full size 60 μM × 60 μM). From left to right Hoechst, Tnp1 staining and Overlay. (**I**–**K**) Images of Tnp2 nuclear distribution in a testis section observed at the same scale as (C)–(H) (full size 60 μM × 60 μM).

when protamines are absent, respectively. In both human and mouse sperm cells from Dpy19l2-dependent globozoospermic males, the retention of histone seemed very important, as suggested by the high rate of sperm (80%) stained by aniline blue (Fig. 5A and B). The protamination of sperm was also strongly defective, with around 60% CMA_3 positive sperm (Fig. 5C and D). The positive results of both compaction tests on globozoospermic mature sperm is in good agreement with the numerous compaction defects characterized above during spermiogenesis. Importantly, these results demonstrate that most of the Dpy19l2-dependent globozoospermic sperm used in ICSI present strong compaction defects in both mouse and human sperm, characterized by a high level of histone retention and low levels of protamination.

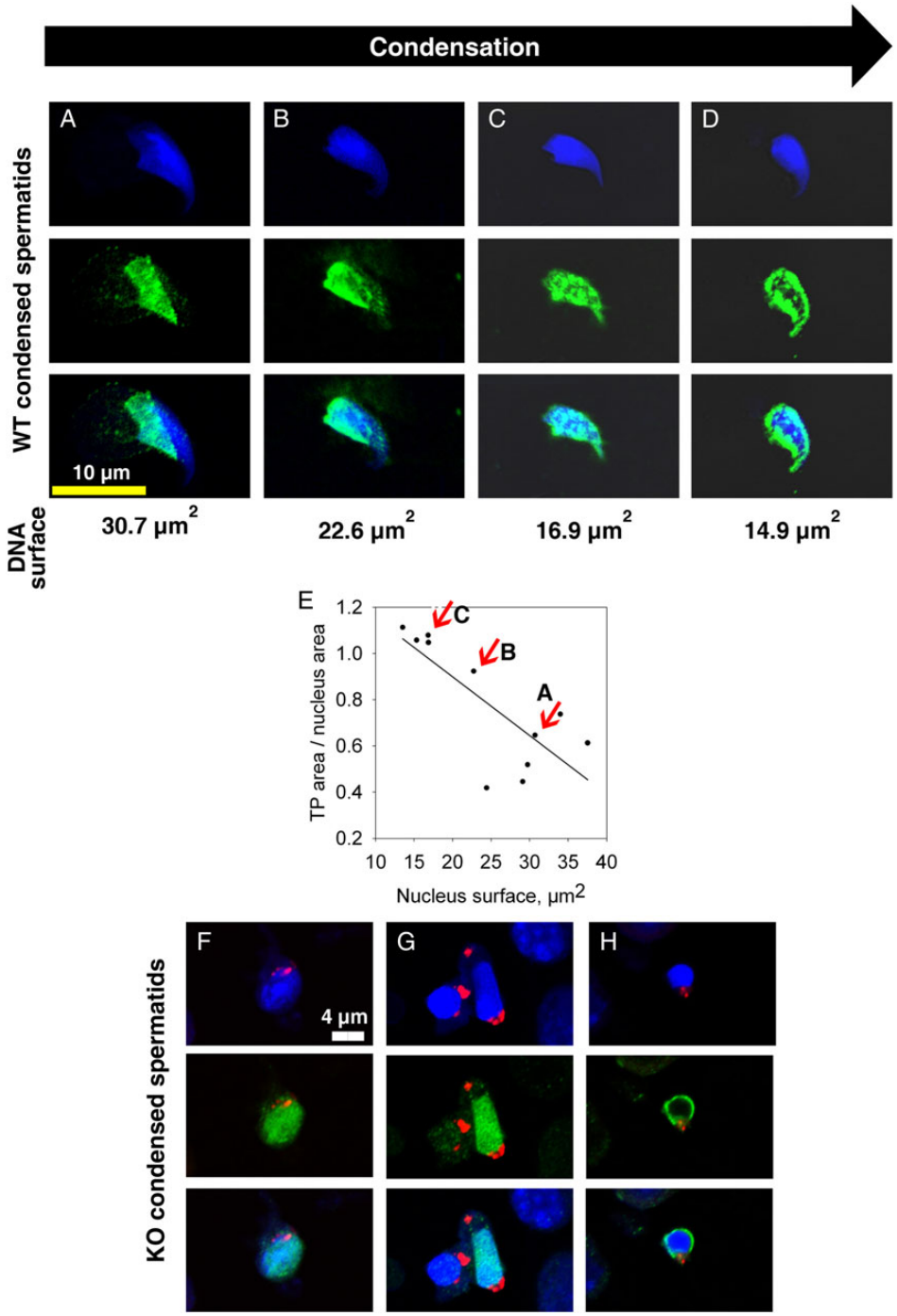

Figure 3 Dynamics of Nuclear Transition Protein Tnp1 during spermatogenesis are different between WT and *Dpy19l2* KO spermatids. (**A**–**D**) Confocal images of WT elongating spermatids showing the dynamics of arrival and removal of Tnp1 transition proteins. Tnp1 proteins invade the spermatid nucleus from the posterior pole (A and B) and then occupy the whole nucleus (C). Tnp1 is removed according to the centrifugal axis (D). From top to bottom: Hoechst, Tnp1 (green) and overlay. (**E**) Graph showing that spermatid condensation is associated with nuclear invasion of TP1. (**F**–**H**) Confocal images of *Dpy19l2* KO elongating spermatids showing the dynamics of arrival and removal of transition proteins. No Tnp1 wave arriving from the posterior pole was observed. Condensed spermatids were homogenously stained with Tnp1 antibodies (F and G), in contrast to WT spermatids. At the end of condensation, a perinuclear ring of Tnp1 staining was observed. DNA is marked with Hoechst (blue), acrosome with sp56 Ab (red) and Tnp1 is stained in green.

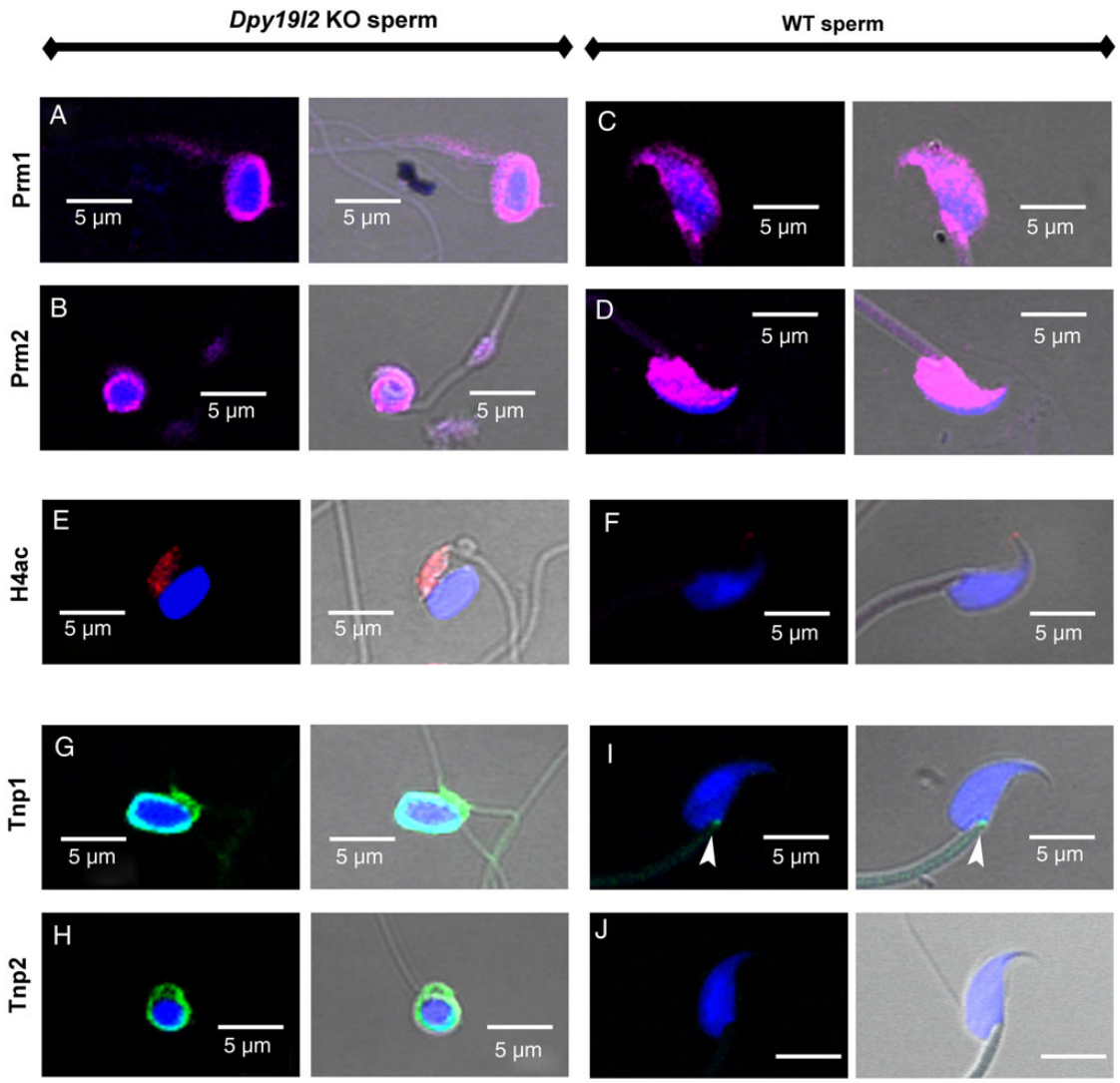

Figure 4 Globozoospermic epididymal sperm present a defective organization of nuclear proteins. (**A**–**D**) Prm1 and Prm2 are the main nuclear proteins of the WT sperm and are present in the whole nucleus (C and D), whereas these proteins are located at the periphery of sperm nuclei only (A and B), in *Dpy19l2* KO globozoospermic sperm. (**E** and **F**) H4ac is absent in WT sperm (F), whereas H4ac is present in the midpiece of the *Dpy19l2* KO sperm (E). (**G**–**J**) Tnp1 and Tnp2 are absent in WT sperm (I and J), whereas they are still present in globozoospermic sperm as a ring structure surrounding the compacted DNA (G and H). First and third columns, overlay of Hoechst and the different protein stainings; Second and fourth columns overlay of Hoechst, the different protein staining and phase contrast.

Absence of protamines increases DNA fragmentation but not oxidative damage during epididymal transit

Sperm DNA compaction based on histone replacement by protamine is further enhanced and stabilized during epididymal maturation by disulfide cross-linking of thiol-rich protamines, allowing paternal genome to be protected from exogenous oxidative stress during sperm storage in the cauda epididymis between two ejaculations and during migration of sperm in the female tract. This disulfide cross-linking involves reactive oxygen species (ROS), produced by the epididymal epithelium. However, ROS also have a detrimental action on sperm lipids and DNA, and the dramatic lack of protamines in *Dpy19l2* KO sperm could increase sperm sensitivity to the stress met during epididymal transit. To test this hypothesis, we measured both DNA fragmentation and oxidative damage in sperm retrieved from the caput to the cauda epididymis. DNA fragmentation was assessed with the TUNEL test and was clearly increased in the spermatozoa from both patients and *Dpy19l2* KO mice in comparison to controls. Human and mouse globozoospermic sperm had a similar percentage of TUNEL positive cells (around 30%, Fig. 6A and B). Interestingly, the level of fragmentation was already high in the caput epididymis and increased only slightly during epididymal transit (from 23.5 $\pm$ 6 to 29 $\pm$ 5%, $n = 2$, Fig. 6C), suggesting that the majority of DNA breaks occur during spermatogenesis. Because DNA

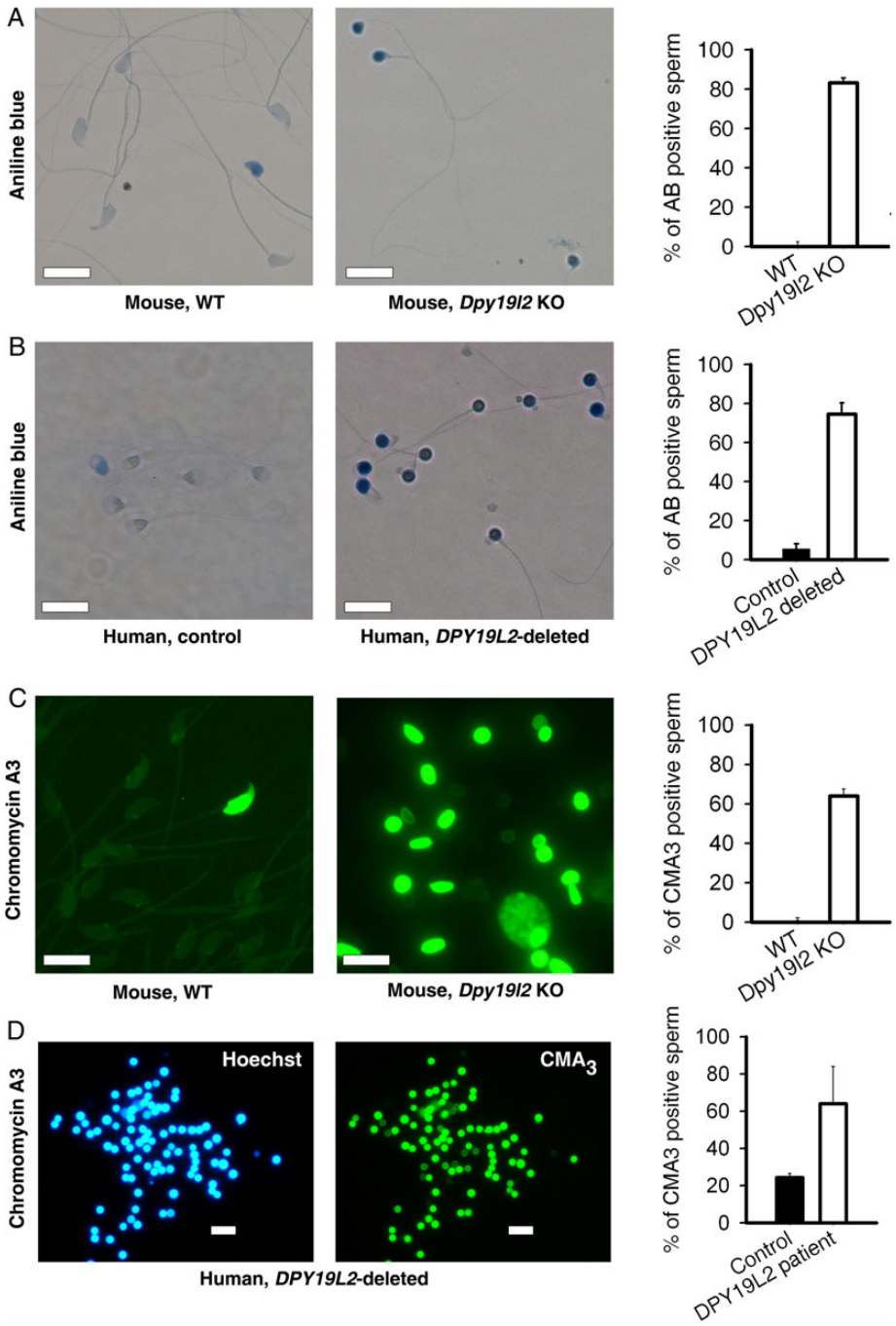

Figure 5 Compaction of DNA is defective in both *Dpy19l2* KO murine sperm and *DPY19L2*-deleted human sperm. (**A**) Mouse sperm were stained with aniline blue. Unlike WT sperm (left), sperm from *Dpy19l2* KO males were strongly stained (middle). The histogram shows the % of stained cells in WT and *Dpy19l2* KO sperm, $n = 3$ (right). There was a significant difference between WT and KO sperm ($P < 0.001$). Bars represent mean ± SE. (**B**) Similar experiments performed with control human sperm and sperm from *DPY19L2*-deleted patients ($n = 3$). The difference was significant ($P < 0.001$). Bars represent mean ± SE. (**C**) Mouse sperm were stained with chromomycin A3. In contrast to WT sperm (left), sperm from *Dpy19l2* KO males were strongly stained (middle). The histogram shows the % of stained cells in WT and *Dpy19l2* KO sperm, $n = 3$ (right). There was a significant difference between WT and KO sperm ($P < 0.001$). Bars represent mean ± SE. (**D**) *DPY19L2*-deleted human sperm were stained with chromomycin A3. The histogram shows the % of stained cells in control and *DPY19L2*-deleted subjects sperm, $n = 3$ (right). The difference was significant ($P = 0.003$). Bars represent mean ± SE.

breaks occur physiologically during spermatogenesis, and histone γH2Ax is involved in the repair process (Leduc *et al.*, 2008), we measured the occurrence of γH2Ax in tubule sections by immunohistochemistry in mouse. We did not observe any obvious difference between WT and *Dpy19l2* KO sperm (Fig. 6D), suggesting that the repair pathways are activated, but may be saturated because sperm in the

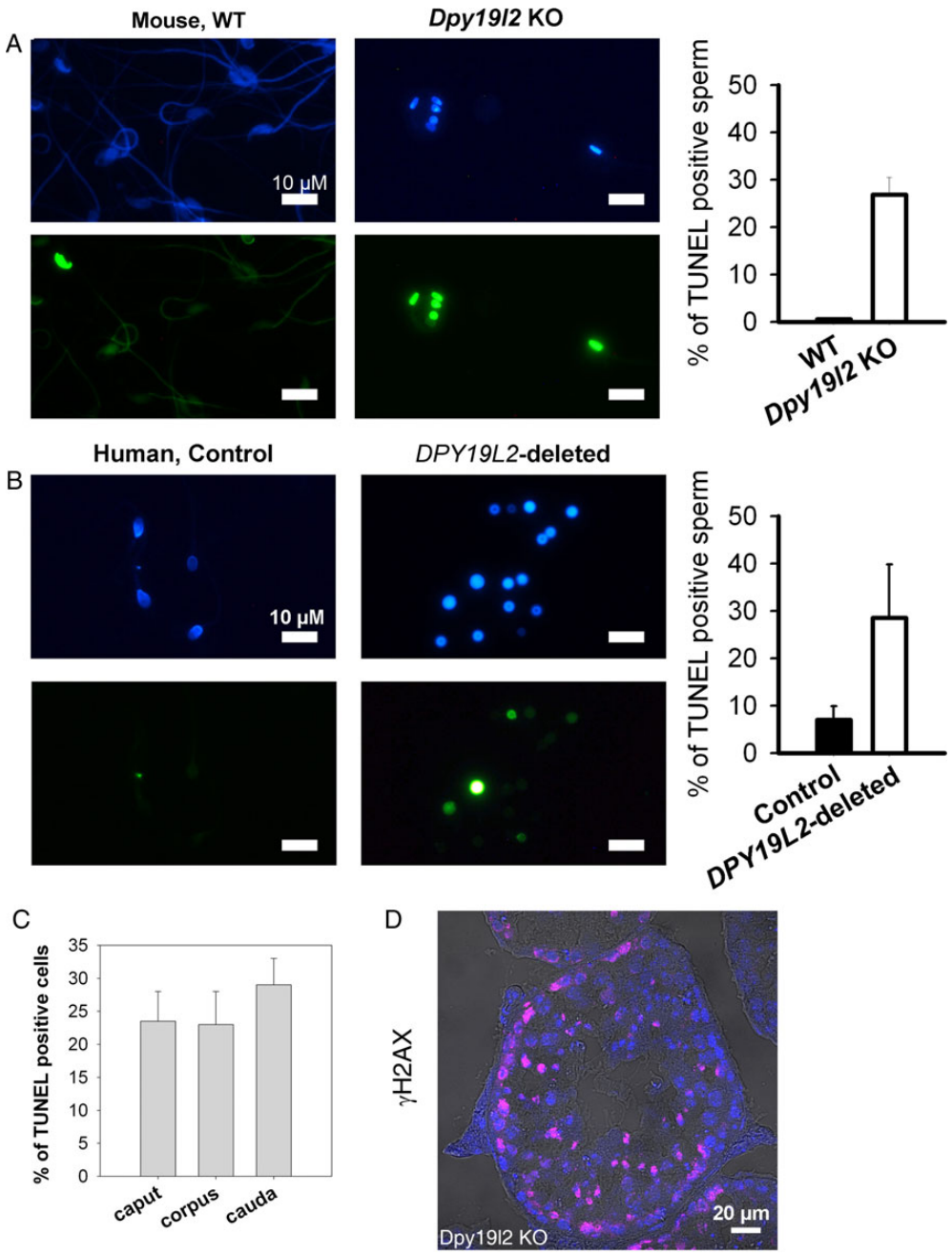

Figure 6 DNA of *Dpy19l2*-dependent globozoospermic sperm is fragmented in mouse and human. (**A**) DNA fragmentation analysis with terminal deoxynucleotidyltransferase-mediated dUTP nick-end labeling (TUNEL) assay. Left, Hoechst and TUNEL stainings in WT sperm. Right, Hoechst and TUNEL stainings in *Dpy19l2* KO sperm. The histogram shows the level of TUNEL positive cells in WT and KO sperm ($n = 5$). There was a significant difference between WT and KO sperm ($P < 0.001$). Bars represent mean ± SE. (**B**) Similar experiments with control and *DPY19L2*-deleted sperm in human. Histogram shows the level of TUNEL positive cells in control ($n = 5$) and *DPY19L2*-deleted sperm ($n = 3$). There was a significant difference between control and *DPY19L2*-deleted sperm ($P = 0.01$). Bars represent mean ± SE. (**C**) Fragmentation of sperm is slightly increased during epididymal transit ($n = 2$). (**D**) Gamma H2AX histone is expressed during spermatogenesis in tubule sections from *Dpy19l2* KO testis.

caput were already damaged. The oxidative status of 8-OHdG from epididymal sperm was also compared by isotope dilution high-performance liquid chromatography-electrospray tandem mass spectrometry assay. The level of 8-OHdG in WT was similar to previously measured levels of 8-OHdG (Badouard *et al.*, 2008) but, unexpectedly, no difference was observed between WT and *Dpy19l2* KO sperm (Fig. 7).

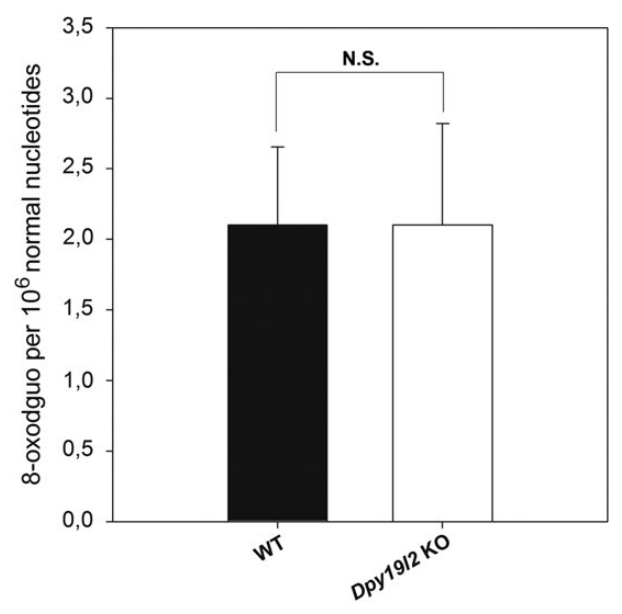

Figure 7 Defective protamination does not lead to a higher level of 8-oxodGuo. Levels of 8-oxo-7,8-dihydro-29-deoxyguanosine (8-oxodGuo) were detected with reversed-phase liquid chromatographic separation associated with an electrospray tandem mass spectrometric detection from epididymal sperm from WT or *Dpy19l2* KO males ($n = 3$). No significant differences were observed between WT and *Dpy19l2* KO males. Bars represent mean ± SE.

Co-injection of PLCζ with *Dpy19l2* KO globozoospermic sperm rescues OA but not embryonic development

Dpy19l2 KO globozoospermic sperm lack PLCζ and its co-injection was expected to rescue OA and thus embryo development. We first verified the ability of PLCζ to trigger OA by injecting PLCζ cRNA into oocytes incubated with cytochalasin B (CB). CB, which blocks extrusion of the second polar body, allows the generation of diploid (2N) parthenogenotes that show better embryonic development than 1N parthenogenetic embryos (Ma *et al.*, 2005). We also validated Sr^{2+}, a common parthenogenetic agent, by incubating CB-treated oocytes in M16 medium containing 10 mM Sr^{2+}. As expected, both compounds triggered OA and initiated high rates of embryonic development up to the blastocyst stage (Fig. 8A); this is unlikely due to exposure to CB alone, which failed by itself to induce OA and/or development.

We next performed ICSI with globozoospermic *Dpy19l2* KO sperm together with Sr^{2+} or PLCζ AOA and monitored preimplantation development. As expected, injection of a *Dpy19l2* KO sperm head failed to trigger OA (Fig. 8B, black bars). In contrast, injection of PLCζ cRNA rescued the activation defect of *Dpy19l2* KO sperm and generated ~60% of 2 PN zygotes (Fig. 8B, green bars). Despite these results, embryo development was highly defective with very few embryos reaching the blastocyst stage. Similar results were observed after ICSI with *Dpy19l2* KO sperm heads followed by Sr^{2+} incubation (Fig. 8B, red bars) and this was despite the fact that Sr^{2+} incubation induced robust Ca^{2+} responses (Fig. 8C). Together, these results demonstrate that, besides the activation defect, Dpy19l2-deficient sperm carry other abnormalities that limit their developmental potential.

Subjects with the *DPY19L2*-deleted gene combine a low OA rate and a poor embryo development

The results obtained in mouse show that embryonic development is strongly compromised when embryos are generated by ICSI with a Dpy19l2-dependent globozoospermic sperm. In human, several teams reported pregnancy with globozoospermic sperm suggesting that embryonic development is less affected than in mouse. In order to evaluate embryo development in human, embryos were scored before implantation at Day 2 or Day 3. Ten embryos obtained following 13 stimulation cycles with 9 males presenting with type I globozoospermia were scored. Although all embryos started their cellular divisions (except for patient T5.1, 3/10), only 2/10 embryos were scored grade I at Day 2 or Day 3 (even blastomeres, fragmentation <10%, Table I), showing that embryonic development is affected in human as well. Finally, the rate of women who gave birth/number of couples with embryos was 28.5% (2/7).

In globozoospermic patients, the ICSI outcome is highly variable, with some medical teams reporting high pregnancy rates and others reporting low fertilization rates, early abortion and finally an absence of delivery. We wondered if this discrepancy between different medical teams could be due to differences in the presence of an acrosome bud and/or DNA quality. For this purpose, we compared two couples, one with successful delivery at the first stimulation cycle and one with unsuccessful ICSI attempts after three stimulation cycles (Table I). Both couples presented a very low rate of OA (0–14%), in accord with the nearly complete absence of PLCζ in the corresponding male (companion article, Escoffier *et al.*, 2014, Fig. 3). Nevertheless, some oocytes could be activated in the absence of AOA (prohibited in France) and 2 embryos were obtained and transferred on Day 3 for one couple. For couple G1, one embryo could be obtained upon the realization of three cycles but could not be transferred due to ovarian hyperstimulation. All embryos were characterized by low grade and high fragmentation levels. We did not measure any difference in the aniline blue and TUNEL stainings, showing that these parameters are not good prognostic markers of successful pregnancy. A difference between CMA_3 rate was observed, but due to the low number of cases, no conclusion could be drawn (Table II).

Discussion

Our recent work demonstrated that the *DPY19L2* gene is the main genetic cause of human globozoospermia (Ben Khelifa *et al.*, 2011; Coutton *et al.*, 2012, 2013). Remarkably, we also showed that the loss of this gene phenocopies globozoospermia in mice (Pierre *et al.*, 2012) and this KO animal model thus represents an interesting tool to investigate the defective molecular process associated with the loss of Dpy19l2 protein during spermatogenesis, because there is no possibility to use human testis for such studies. Dpy19l2-dependent globozoospermia is characterized by the absence of an acrosome, preventing the sperm from crossing the *zona pellucida*, and represents the first reason for the sperm infertility. We have shown in the accompanying paper that the defective acrosomal

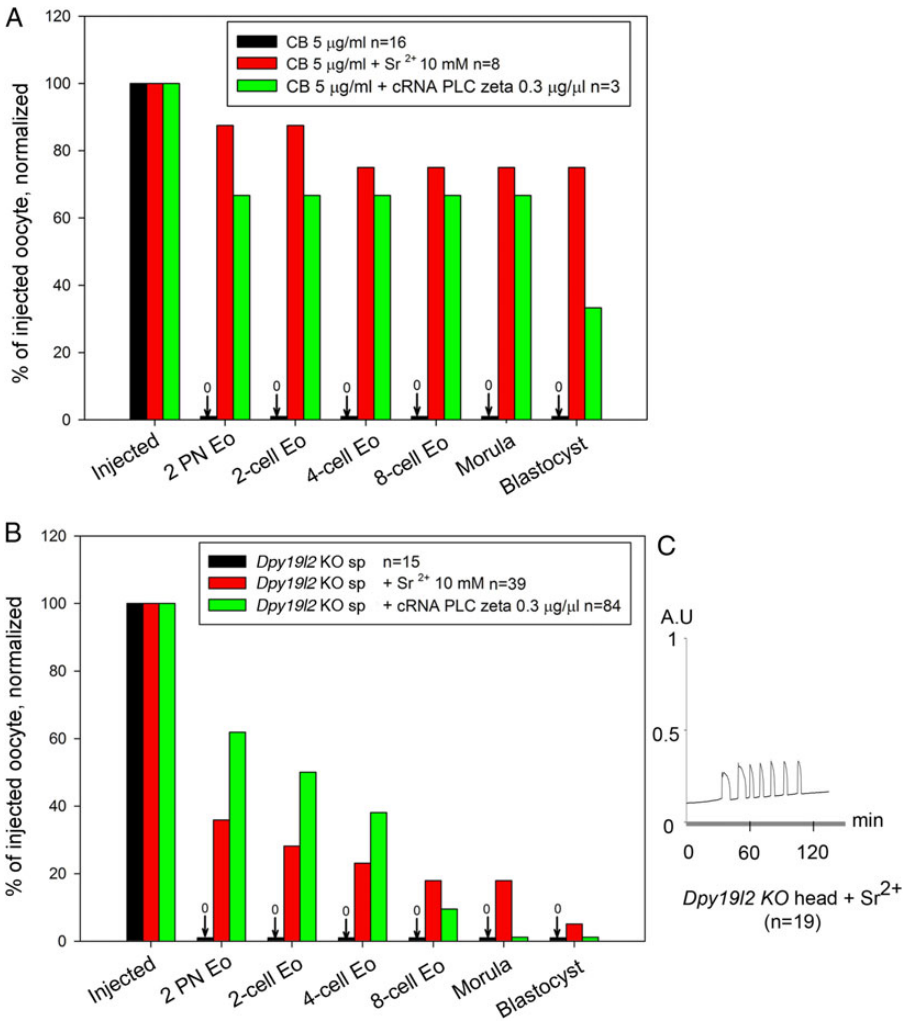

Figure 8 Rescue of oocyte activation with PLCζ cRNA injection in ICSI performed with *Dpy19l2* KO sperm does not allow recovery of full embryo development. (**A**) In the presence of cytochalasin B (CB), both strontium (Sr^{2+}) incubation (red bars) and phospholipase C (PLCζ) cRNA injection (green bars) were able to induce full oocyte activation, allowing parthenogenetic development of embryos up to the blastocyst stage. Incubation of oocytes with CB only does not activate the oocyte (black bars). *n* corresponds to the number of challenged oocytes (for CB or CB + Sr^{2+}) or injected oocytes that survived the ICSI procedure (CB + cRNA and Dpy19l2 KO sperm injection). (**B**) *Dpy19l2* KO sperm heads were either injected in MII oocytes and embryos were incubated in the presence of Sr^{2+} for 2 h (red bars) or *Dpy19l2* KO sperm heads were co-injected with PLCζ cRNA in MII oocytes (green bars). In contrast to CB treatment, injection of *Dpy19l2* KO sperm head is associated with poor blastocyst outcomes in both activation conditions. (**C**) Sr^{2+} incubation induced a robust Ca^{2+} response. AU: arbitrary units.

biogenesis leads to loss of the sperm factor PLCζ as well, making worse the sterility phenotype of these sperm due to the absence of OA. Herein, we describe for the first time the main stages of spermatid condensation in globozoospermic sperm and pin pointed that several stages are defective, which render this sperm more susceptible to DNA defects and that ultimately undermine the developmental potential of zygotes generated using globozoospermic sperm. We thus demonstrated a third molecular cause of sterility associated with globozoospermia. We also noted some differences in phenotype of the disease between human and mice. We indeed showed that the phenotype in the mouse, in terms of embryonic developmental capacity, is more severe than in men.

Impact of defective DNA condensation of globozoospermic sperm on embryonic development

Previous reports have shown that globozoospermic sperm present defects in condensation, which is likely associated with the increased percentage of DNA fragmentation reported in these types of sperm. Nevertheless, the level of DNA fragmentation reported is quite different between studies with rates ranging from 10 to 37% (Baccetti *et al.*, 1996; Vicari *et al.*, 2002). Importantly, the etiology of these DNA defects in sperm remains unknown. Herein, we showed that defects in several steps of sperm head condensation occur in globozoospermic

Table I **ICSI outcomes following 13 stimulation cycles with 9 males presenting with type I globozoospermia due to full deletion of the *DPY19L2* gene.**

Patient ID	Age male years	Age female years	Nber MII oocyte (%)	Nber 2 PN embryo (%)	TRANSFER day 2 (D2)		TRANSFER D3		Grade of embryo	Nber of transferred Eo (D2)	Nber of transferred Eo (D3)	Delivery
					Nber of embryos at D2	Quality and % of fragmentation	Nber of embryos at D3	Quality and % of fragmentation				
M1	30	28	14	2			2			0	2	1
				(14.3%)				- 6-cell, 10–30% fragmentation	G III			
								- 6-cell, 30–50% fragmentation	G III			
G1-1	37	29	10	1			1			0	0	0
				(10%)				- 5-cell, 10–30% fragmentation	G III			
G1-2	37	29	4	0			0			0	0	0
				(0%)								
G1-3	38	30	5	0			0			0	0	0
				(0%)								
T1.1	31	27	10	0			0			0	0	
				(0%)								
T1.2	40	36	6	0			0			0	0	
T3	50	37	8	0			0			0	0	
				(0%)								
T4	40	36	4	0			0			0	0	
T5.1	36	24	29	10	3					3	0	0
				(34.5%)		- 5-cell, 0% fragmentation			G II			
						- 5-cell, 0% fragmentation			G II			
						- 8-cell, 15% fragmentation			G III			
T5.2	38	26	19	1			1			0	1	0
				(5.3%)				- 4-cell, 10% fragmentation	G II			
T7	30	26	10	1			1			0	0	0
				(10%)				- 2-cell (Development delayed)	G IV			
T8	42	35	11	1			1			0	1	0
				(9%)				- 8-cell, 0% fragmentation	G I			
T9	38	28	9	1	1					1	0	1
				(11.1%)		- 4-cell, 10% fragmentation			G I			

Nber (number), Eo (Embryo). MII: metaphase II oocytes retrieved; PN: pronuclei.

Table II **Medical history, laboratory investigations and ICSI outcomes of two couples with males presenting with type I globozoospermia due to full deletion of the *DPY19L2* gene.**

Patient ID	Age male years	Age female years	History/ habits	Volume ejaculate [sperm]	Sperm mobility	% of globozoospermia	Genotyping	TUNEL % Positive	AB % positive	CMA3 % positive	Nber MII oocytes (%)	Nber 2 PN embryos (%)	Nber of embryos at D3	Quality and grade of embryos	Nber of transferred Eo (D3)	Delivery
M1	30	28	Tobacco	4.8 ml	20% a + b	100%	*DPY19L2* deleted homoz	29	81.5	50	14	2	**2**		2	1
			5–10 cig/d	21 M/ml	20% c							(14.3%)		- 6-cell, 10–30% fragment (G III)		
			Bricklayer											- 6-cell, 30–50% fragment (G III)		
G1-1	37	29	Tobacco	3.2 ml	30% a + b	100%	*DPY19L2* deleted homoz	44	79	ND	10	1	**1**		0	0
			15 cig/d	28 M/ml								(10%)		- 5-cell, 10–30% fragment (G III)		
			Cannabis 2/D													
G1-2	37	29	Tobacco	2 ml	20%a + b	100%	*DPY19L2* deleted homoz	ND	ND	ND	4	0	0		0	0
			15 cig/d	30 M/ml	10%c							(0%)				
			Cannabis 2/D													
G1-3	38	30	Tobacco	2.5 ml	20% a + b	100%	*DPY19L2* deleted homoz	18	79	78	5	0	0		0	0
			5 cig/d	20 M/ml	5%c							(0%)				
			Cannabis 3/w													

ND: not determined; cig/day: cigarettes per day; TUNEL: terminal deoxynucleotidyltransferase-mediated dUTP nick-end labeling; AB: aniline blue; CMA3: chromomycin A_3; MII: metaphase II oocytes retrieved; PN: pronuclei.

sperm. For instance, during the initial stages of condensation in stage X, the disappearance of acetylated H4 is greatly modified, with WT sperm preserving acetylated H4 histones in the posterior or base of the sperm head, a pattern that was not observed in *Dpy19l2* KO sperm, which presented a uniform, circular pattern of H4 distribution. Similarly, the dynamic of arrival of Tnps is different, following a postero-anterior axis with WT sperm, an axis which was not present in *Dpy19l2* KO sperm. Lastly, the defect associated with protamination is very pronounced in *Dpy19l2* KO sperm, as in these cells protamines were absent inside the nucleus and remained mostly located at the periphery. Together, these defects are likely to impact the developmental potential of embryos generated with globozoospermic sperm. Indeed, recent data show that the paternal genome and epigenome play crucial roles in embryo development (Jenkins and Carrell, 2012). It is known that parent-specific methylation of promoter regions of imprinted genes is required for successful embryo development as well as the specific organization of the paternal epigenome, which is in part determined by protamination and the retention of nucleosomes at specific loci. Defective protamination is associated with various forms of human infertility, reviewed in (Oliva, 2006) and loci retaining nucleosomes enriched in methylated histone H3 are involved in the developmental process and correspond to imprinted genes, HOX genes and microRNA clusters (Hammoud *et al*., 2009). In late condensing mouse spermatids and sperm, nucleosomes containing testis-specific histone variants H2AL1/L2 remain in pericentric heterochromatin regions, likely guiding the epigenetic reprogramming of these regions (Govin *et al*., 2007). The perturbations of sperm DNA compaction, as witnessed herein by H4ac, Tnp1 and protamine studies, therefore likely lead to major sperm epigenetic defects. Moreover, the perturbations of sperm DNA compaction are likely to increase susceptibility to DNA breaks. Altogether, epigenetic defects and DNA breaks likely undermine the developmental potential of embryos generated by ICSI using *Dpy19l2* KO sperm or human sperm lacking DPY19l2, as showed in this study. Despite its transcriptionally inert state, the sperm nucleus contains diverse RNA populations, mRNAs, and non-coding RNA (ncRNA) that have been transcribed throughout spermatogenesis (Dadoune, 2009). Although the contribution of such sperm RNA to embryonic development or infertility is highly debated, the content of ncRNA in globozoospermic sperm is unknown and may also represent a cause of impaired embryo development.

Interestingly, most of the DNA breaks were already present when sperm reach the epididymis and thus occur inside the testis, during DNA compaction. Moreover, the levels of oxidative damage of WT and *Dpy19l2* KO sperm obtained in the cauda epididymides were quite similar, suggesting that the oxidative stress met during epididymal transit does not modify the overall oxidative status of globozoospermic sperm DNA, which is unexpectedly low for a protamine-deficient sperm. These points are important because several studies showed that testicular sperm have a better developmental potential than epididymal sperm in the case of oligo-terato-asthenozoospermia (Weissman *et al*., 2008; Ben-Ami *et al*., 2013). Our results suggest that testicular sperm extraction in Dpy19l2-dependent globozoospermia is not recommended.

Difference between human and mouse embryonic development

The compromised development of embryos generated by globozoospermic sperm and ICSI and activated by PLCζ is more severe in mouse than in humans. In the murine species, <15.4% of the zygotes reached the 8-cell stage and only 1.9% reached the blastocyst stage; this developmental failure cannot be due to an activation defect or the dose of PLCζ (Yu *et al*., 2008), as CB treated oocytes activated and developed to blastocyst stage with the same dose of PLCζ. In contrast, most of the 2-PN human zygotes reached the 8-cell stage, at which time they were transferred. Nevertheless, it is important to note that these human embryos displayed high levels of fragmentation and were mostly given low grades during the evaluation. The rate of grade I embryos is very low (20%) in comparison to that reported for couples with a tuboperitoneal female factor only and normal spermatogram (~50%), a report using the same embryo gradation system (Bukulmez *et al*., 2000). In spite of this, embryos implanted, developed and two offspring was produced, which is in agreement with previously published results (28 versus 31% in (Kuentz *et al*., 2013)). It is nevertheless difficult to compare both methods because the number of couples studied in this report is low. Moreover, it is important to stress that these rates are low for young women, compared with a 45.9% (age <35 years) delivery rate in a large study of control cohort patients (Palermo *et al*., 2009), underlining that human embryos generated with globozoospermic sperm have a compromised development as well. A possible explanation for the different developmental potential between zygotes generated by human or mouse globozoospermic sperm is the degree of nucleosome replacement by protamines during spermatogenesis. Whereas protamination is almost complete in mouse sperm and the presence of nucleosomes associated with DNA is estimated to be ~1%, in humans this is estimated to be ~10–15% (Bench *et al*., 1996; van der Heijden *et al*., 2008). We speculate therefore that the reduced level of protamines, which is observed in globozoospermic sperm, may be better tolerated by human sperm than by mouse sperm or that human oocytes are more able to overcome/repair these defects, or a combination of both possibilities, explaining the better developmental potential of human zygotes generated with globozoospermic sperm. It is worth noting that the higher rate of embryonic development arrest observed in the mouse is not due to a differential disruption of the paternal centrosome because mouse sperm are devoid of centrioles and key centrosomal components, and the first mitotic spindle actually depends on the maternal centrosomal material (Schatten *et al*., 1986). The relationship between fertilization or embryo development and DNA damage was clearly demonstrated in animal models (Ahmadi and Ng, 1999; Fatehi *et al*., 2006), but this question is more debated in human reproduction, where no linear correlation between sperm DNA damage and pregnancy outcome was clearly shown (Sakkas *et al*., 1998). The absence of a clear correlation is partly due to i) an absence of a thorough characterization of chromatin defects and DNA damage, due to the use of simple and basic tests and ii) an absence of statistical analysis of the fate of each embryo generated by ICSI because in human only one pregnancy per oocyte cohort is sought, allowing selection of the best embryos (Sakkas and Alvarez, 2010). In the framework of type I globozoospermia, human data, reinforced by those obtained with the *Dpy19l2* KO model, enabled us to show that defective compaction, and more particularly protamination, associated with DNA breaks strongly impairs the developmental potential of embryos generated by ICSI using *Dpy19l2*-deficient sperm.

In conclusion, in this study we describe for the first time chromatin condensation during mouse spermatogenesis of Dpy19l2-dependent globozoospermic males and organization of globozoospermic sperm in mouse and human, showing that important modifications occur, severely

limiting the developmental potential of these gametes. Our results and those of others also show that in spite of this, offspring can be conceived with these 'faulty' sperm. In the mouse, an increasing number of publications show clear health and behavioral alterations in progeny generated by ART even from healthy animals (Ecker *et al*., 2004; Fernandez-Gonzalez *et al*., 2008; Kohda and Ishino, 2013). Further work would require studying the long-term development of mice generated with globozoospermic sperm to assess the long-term effect of DNA breaks and failed compaction. In the meantime we stress that transferring embryos generated by ICSI using incorrectly compacted sperm combined with DNA breaks should be performed with caution. Similar abnormalities are present in most cases of teratozoospermia. It is therefore imperative that we gain insight into the sperm molecular DNA landscapes that are associated with most cases of human infertility. Methods allowing the detection and negative selection of faulty sperm should then be developed to increase ART success rate and to decrease the risks of deleterious effects on offspring health.

Acknowledgements

We are grateful to the patients who gave their informed consent to the use of their samples for research. We thank Saadi Khochbin and Sophie Rousseaux for useful discussions and for critical comments on the manuscript. We also thank clinicians from the reproductive clinics (Pascale Hoffman, Ulrike Bergues, Dr B. Courbière) and C. Metton and M.J. Fays-Bernardin for technical assistance and Germetheque support.

Authors' roles

J.E. performed ICSI experiments. H.C.L. performed calcium imaging experiments. G.M. studied human and mouse DNA defects. S.Y. performed confocal experiments on sperm DNA compaction. R.Z., S.H. and C.M.-G. provided clinical data and human sperm samples. J.-L.R. performed mass spectrometry experiments. C.C. and T.K. were responsible of molecular biology experiments. P.F.R, R.F. and C.A. coordinated the study. P.F.R., R.F. and C.A. contributed to discussion, design and interpretation of data. C.A. wrote the manuscript.

Funding

This study was supported by grants from Gravit Foundation (to C.A.), from the Agence National de la Recherche (Grant ICG2I to P.F.R. and C.A.) from NIH (Grant number: R01 HD051872 to R.F.).

Conflict of interest

None declared.

References

Ahmadi A, Ng SC. Developmental capacity of damaged spermatozoa. *Hum Reprod* 1999;**14**:2279–2285.

Arpanahi A, Brinkworth M, Iles D, Krawetz SA, Paradowska A, Platts AE, Saida M, Steger K, Tedder P, Miller D. Endonuclease-sensitive regions of human spermatozoal chromatin are highly enriched in promoter and CTCF binding sequences. *Genome Res* 2009;**19**:1338–1349.

Baccetti B, Collodel G, Piomboni P. Apoptosis in human ejaculated sperm cells (notulae seminologicae 9). *J Submicrosc Cytol Pathol* 1996; **28**:587–596.

Badouard C, Menezo Y, Panteix G, Ravanat JL, Douki T, Cadet J, Favier A. Determination of new types of DNA lesions in human sperm. *Zygote* 2008;**16**:9–13.

Battaglia DE, Koehler JK, Klein NA, Tucker MJ. Failure of oocyte activation after intracytoplasmic sperm injection using round-headed sperm. *Fertil Steril* 1997;**68**:118–122.

Ben-Ami I, Raziel A, Strassburger D, Komarovsky D, Ron-El R, Friedler S. Intracytoplasmic sperm injection outcome of ejaculated versus extracted testicular spermatozoa in cryptozoospermic men. *Fertil Steril* 2013; **99**:1867–1871.

Bench GS, Friz AM, Corzett MH, Morse DH, Balhorn R. DNA and total protamine masses in individual sperm from fertile mammalian subjects. *Cytometry* 1996;**23**:263–271.

Ben Khelifa M, Zouari R, Harbuz R, Halouani L, Arnoult C, Lunardi J, Ray PF. A new AURKC mutation causing macrozoospermia: implications for human spermatogenesis and clinical diagnosis. *Mol Hum Reprod* 2011; **17**:762–768.

Bukulmez O, Yarali H, Yucel A, Sari T, Gurgan T. Intracytoplasmic sperm injection versus *in vitro* fertilization for patients with a tubal factor as their sole cause of infertility: a prospective, randomized trial. *Fertil Steril* 2000; **73**:38–42.

Cho C, Willis WD, Goulding EH, Jung-Ha H, Choi YC, Hecht NB, Eddy EM. Haploinsufficiency of protamine-1 or -2 causes infertility in mice. *Nat Genet* 2001;**28**:82–86.

Coutton C, Zouari R, Abada F, Ben Khelifa M, Merdassi G, Triki C, Escalier D, Hesters L, Mitchell V, Levy R *et al.* MLPA and sequence analysis of DPY19L2 reveals point mutations causing globozoospermia. *Hum Reprod* 2012;**27**:2549–2558.

Coutton C, Abada F, Karaouzene T, Sanlaville D, Satre V, Lunardi J, Jouk PS, Arnoult C, Thierry-Mieg N, Ray PF. Fine characterisation of a recombination hotspot at the DPY19L2 locus and resolution of the paradoxical excess of duplications over deletions in the general population. *PLoS Genet* 2013;**9**:e1003363.

Dadoune JP. Spermatozoal RNAs: what about their functions? *Microsc Res Tech* 2009;**72**:536–551.

Dam AH, Koscinski I, Kremer JA, Moutou C, Jaeger AS, Oudakker AR, Tournaye H, Charlet N, Lagier-Tourenne C, van Bokhoven H *et al.* Homozygous mutation in SPATA16 is associated with male infertility in human globozoospermia. *Am J Hum Genet* 2007;**81**:813–820.

Ecker DJ, Stein P, Xu Z, Williams CJ, Kopf GS, Bilker WB, Abel T, Schultz RM. Long-term effects of culture of preimplantation mouse embryos on behavior. *Proc Natl Acad Sci USA* 2004;**101**:1595–1600.

Fatehi AN, Bevers MM, Schoevers E, Roelen BA, Colenbrander B, Gadella BM. DNA damage in bovine sperm does not block fertilization and early embryonic development but induces apoptosis after the first cleavages. *J Androl* 2006;**27**:176–188.

Fernandez-Gonzalez R, Moreira PN, Perez-Crespo M, Sanchez-Martin M, Ramirez MA, Pericuesta E, Bilbao A, Bermejo-Alvarez P, de Dios HJ, de Fonseca FR *et al.* Long-term effects of mouse intracytoplasmic sperm injection with DNA-fragmented sperm on health and behavior of adult offspring. *Biol Reprod* 2008;**78**:761–772.

Gaucher J, Boussouar F, Montellier E, Curtet S, Buchou T, Bertrand S, Hery P, Jounier S, Depaux A, Vitte AL *et al.* Bromodomain-dependent stage-specific male genome programming by Brdt. *EMBO J* 2012;**31**: 3809–3820.

Govin J, Escoffier E, Rousseaux S, Kuhn L, Ferro M, Thevenon J, Catena R, Davidson I, Garin J, Khochbin S *et al.* Pericentric heterochromatin reprogramming by new histone variants during mouse spermiogenesis. *J Cell Biol* 2007;**176**:283–294.

Hammoud SS, Nix DA, Zhang H, Purwar J, Carrell DT, Cairns BR. Distinctive chromatin in human sperm packages genes for embryo development. *Nature* 2009;**460**:473–478.

Harbuz R, Zouari R, Pierre V, Ben Khelifa M, Kharouf M, Coutton C, Merdassi G, Abada F, Escoffier J, Nikas Y *et al.* A recurrent deletion of DPY19L2 causes infertility in man by blocking sperm head elongation and acrosome formation. *Am J Hum Genet* 2011;**88**:351–361.

Hazzouri M, Pivot-Pajot C, Faure AK, Usson Y, Pelletier R, Sele B, Khochbin S, Rousseaux S. Regulated hyperacetylation of core histones during mouse spermatogenesis: involvement of histone deacetylases. *Eur J Cell Biol* 2000;**79**:950–960.

Jenkins TG, Carrell DT. The sperm epigenome and potential implications for the developing embryo. *Reproduction* 2012;**143**:727–734.

Kohda T, Ishino F. Embryo manipulation via assisted reproductive technology and epigenetic asymmetry in mammalian early development. *Philos Trans R Soc Lond B Biol Sci* 2013;**368**:20120353.

Kolthur-Seetharam U, Pradeepa MM, Gupta N, Narayanaswamy R, Rao MR. Spatiotemporal organization of AT- and GC-rich DNA and their association with transition proteins TP1 and TP2 in rat condensing spermatids. *J Histochem Cytochem* 2009;**57**:951–962.

Kuentz P, Vanden Meerschaut F, Elinati E, Nasr-Esfahani MH, Gurgan T, Iqbal N, Carre-Pigeon F, Brugnon F, Gitlin SA, Velez dlC *et al.* Assisted oocyte activation overcomes fertilization failure in globozoospermic patients regardless of the DPY19L2 status. *Hum Reprod* 2013;**28**:1054–1061.

Kyono K, Nakajo Y, Nishinaka C, Hattori H, Kyoya T, Ishikawa T, Abe H, Araki Y. A birth from the transfer of a single vitrified-warmed blastocyst using intracytoplasmic sperm injection with calcium ionophore oocyte activation in a globozoospermic patient. *Fertil Steril* 2009;**91**:931–911.

Leduc F, Maquennehan V, Nkoma GB, Boissonneault G. DNA damage response during chromatin remodeling in elongating spermatids of mice. *Biol Reprod* 2008;**78**:324–332.

Liu J, Nagy Z, Joris H, Tournaye H, Devroey P, Van SA. Successful fertilization and establishment of pregnancies after intracytoplasmic sperm injection in patients with globozoospermia. *Hum Reprod* 1995;**10**:626–629.

Liu G, Shi QW, Lu GX. A newly discovered mutation in PICK1 in a human with globozoospermia. *Asian J Androl* 2010;**12**:556–560.

Lundin K, Sjogren A, Nilsson L, Hamberger L. Fertilization and pregnancy after intracytoplasmic microinjection of acrosomeless spermatozoa. *Fertil Steril* 1994;**62**:1266–1267.

Ma SF, Liu XY, Miao DQ, Han ZB, Zhang X, Miao YL, Yanagimachi R, Tan JH. Parthenogenetic activation of mouse oocytes by strontium chloride: a search for the best conditions. *Theriogenology* 2005;**64**:1142–1157.

Miller D, Brinkworth M, Iles D. Paternal DNA packaging in spermatozoa: more than the sum of its parts? DNA, histones, protamines and epigenetics. *Reproduction* 2010;**139**:287–301.

Montellier E, Boussouar F, Rousseaux S, Zhang K, Buchou T, Fenaille F, Shiota H, Debernardi A, Hery P, Curtet S *et al.* Chromatin-to-nucleoprotamine transition is controlled by the histone H2B variant TH2B. *Genes Dev* 2013;**27**:1680–1692.

Oliva R. Protamines and male infertility. *Hum Reprod Update* 2006;**12**:417–435.

Palermo GD, Neri QV, Takeuchi T, Rosenwaks Z. ICSI: where we have been and where we are going. *Semin Reprod Med* 2009;**27**:191–201.

Pierre V, Martinez G, Coutton C, Delaroche J, Yassine S, Novella C, Pernet-Gallay K, Hennebicq S, Ray PF, Arnoult C. Absence of Dpy19l2, a new inner nuclear membrane protein, causes globozoospermia in mice by preventing the anchoring of the acrosome to the nucleus. *Development* 2012;**139**:2955–2965.

Ravanat JL, Duretz B, Guiller A, Douki T, Cadet J. Isotope dilution high-performance liquid chromatography-electrospray tandem mass spectrometry assay for the measurement of 8-oxo-7,8-dihydro-2′-deoxyguanosine in biological samples. *J Chromatogr B Biomed Sci Appl* 1998;**715**:349–356.

Sakkas D, Alvarez JG. Sperm DNA fragmentation: mechanisms of origin, impact on reproductive outcome, and analysis. *Fertil Steril* 2010; **93**:1027–1036.

Sakkas D, Urner F, Bizzaro D, Manicardi G, Bianchi PG, Shoukir Y, Campana A. Sperm nuclear DNA damage and altered chromatin structure: effect on fertilization and embryo development. *Hum Reprod* 1998;**13**(Suppl 4):11–19. 11–19.

Schatten H, Schatten G, Mazia D, Balczon R, Simerly C. Behavior of centrosomes during fertilization and cell division in mouse oocytes and in sea urchin eggs. *Proc Natl Acad Sci USA* 1986;**83**:105–109.

Taylor SL, Yoon SY, Morshedi MS, Lacey DR, Jellerette T, Fissore RA, Oehninger S. Complete globozoospermia associated with PLCzeta deficiency treated with calcium ionophore and ICSI results in pregnancy. *Reprod Biomed Online* 2010;**20**:559–564.

Tejera A, Molla M, Muriel L, Remohi J, Pellicer A, De Pablo JL. Successful pregnancy and childbirth after intracytoplasmic sperm injection with calcium ionophore oocyte activation in a globozoospermic patient. *Fertil Steril* 2008;**90**:1202–1205.

van der Heijden GW, Ramos L, Baart EB, van den Berg IM, Derijck AA, vand V, Martini E, de Boer BP. Sperm-derived histones contribute to zygotic chromatin in humans. *BMC Dev Biol* 2008;**8**:34. doi: 10.1186/1471-213X-8-34., 34-38.

Vicari E, Perdichizzi A, De PA, Burrello N, D'Agata R, Calogero AE. Globozoospermia is associated with chromatin structure abnormalities: case report. *Hum Reprod* 2002;**17**:2128–2133.

Vozdova M, Rybar R, Kloudova S, Prinosilova P, Texl P, Rubes J. Total globozoospermia associated with increased frequency of immature spermatozoa with chromatin defects and aneuploidy: a case report. *Andrologia* 2013;**10**:00–00.

Weissman A, Horowitz E, Ravhon A, Nahum H, Golan A, Levran D. Pregnancies and live births following ICSI with testicular spermatozoa after repeated implantation failure using ejaculated spermatozoa. *Reprod Biomed Online* 2008;**17**:605–609.

Yoshida N, Perry AC. Piezo-actuated mouse intracytoplasmic sperm injection (ICSI). *Nat Protoc* 2007;**2**:296–304.

Yu Y, Saunders CM, Lai FA, Swann K. Preimplantation development of mouse oocytes activated by different levels of human phospholipase C zeta. *Hum Reprod* 2008;**23**:365–373.

Zhao M, Shirley CR, Hayashi S, Marcon L, Mohapatra B, Suganuma R, Behringer RR, Boissonneault G, Yanagimachi R, Meistrich ML. Transition nuclear proteins are required for normal chromatin condensation and functional sperm development. *Genesis* 2004;**38**:200–213.